JOC The Journal of Organic Chemistry

Article

pubs.acs.org/joc

Cyclohexane-Fused Octahydroquinolizine Alkaloids from *Myrioneuron faberi* with Activity against Hepatitis C Virus

Ming-Ming Cao,[†,‡] Yu Zhang,[†] Xiao-Hui Li,[†,‡] Zong-Gen Peng,[§] Jian-Dong Jiang,[§] Yu-Cheng Gu,[∥] Ying-Tong Di,[†] Xiao-Nian Li,[†] Duo-Zhi Chen,[†] Cheng-Feng Xia,[†] Hong-Ping He,[†] Shun-Lin Li,[†] and Xiao-Jiang Hao*

[†]State Key Laboratory of Phytochemistry and Plant Resources in West China, Kunming Institute of Botany, Chinese Academy of Sciences, Kunming 650201, Yunnan, People's Republic of China

[‡]Graduate School of the Chinese Academy of Sciences, Beijing 100039, People's Republic of China

[§]Institute of Medicinal Biotechnology, Chinese Academy of Medical Sciences and Peking Union Medical College, Beijing 10050, People's Republic of China

[∥]Syngenta, Jealott's Hill International Research Centre, Bracknell, Berkshire RG42 6EY, U.K.

Supporting Information

ABSTRACT: Investigation of the alkaloids from *Myrioneuron faberi*, a plant unique to China, gave four pairs of enantiomers (**1**−**4**). (±)-*β*-Myrifabral A (**1**) and (±)-*α*-myrifabral A (**2**) formed an inseparable mixture of anomers (cluster A), as did (±)-*β*-myrifabral B (**3**) and (±)-*α*-myrifabral B (**4**) (cluster B). Their structures were determined by X-ray diffraction and NMR analysis. Compounds **1**−**4** possessed novel cyclohexane-fused octahydroquinolizine skeletons and represent the first quinolizidine alkaloids from the genus *Myrioneuron*. The epimers of cluster A (**1** and **2**) were modified and separated. In vitro, clusters A and B and their derivatives inhibited replication of hepatitis C virus (HCV, IC_{50} 0.9 to 4.7 μM) with cytotoxicity lower than that of telaprevir.

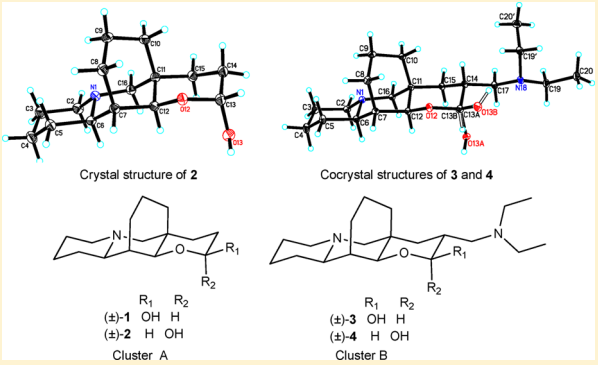

INTRODUCTION

Hepatitis C virus (HCV) infection is a worldwide health problem, as approximately 130−150 million people are infected according to the World Health Organization.[1] One present therapy for HCV infection is a combination of interferon and nucleotide analogue, which are associated with significant side effects[2] and the development of resistance.[3] One promising nucleotide analogue for HCV infection is sovaldi, which is a genotype-specific and all-oral nucleotide analogue and can be used without interferon.[4] Nucleotide analogue inhibitors may result in drug-resistant mutant strains, and new inhibitors are urgently required.[5] Natural product libraries are useful sources of potential drugs.[6] Thus, continuing the search for anti-HCV compounds, especially those derived from natural products as an alternative way, is desirable.

Myrioneuron alkaloids are a newly discovered family of structurally diverse natural products derived from lysine featuring polycyclic ring systems (tri-, tetra-, penta-, hexa-, and decacyclic) are produced by plants in the genus *Myrioneuron* R. Br. (Rubiaceae).[7] Some of them inhibit KB cell proliferation, while others exhibit remarkable antimalarial, antimicrobial, and anti-HCV activities.[7c−g]

To continue our investigations of anti-HCV *Myrioneuron* alkaloids,[7f,g] four pairs of enantiomers (**1**−**4**) were isolated from *Myrioneuron faberi*, and their structures were determined unambiguously by X-ray diffraction analysis. All previously known *Myrioneuron* alkaloids feature the decahydroquinoline (DHQ) motif; however, **1**−**4** possess a novel cyclohexane-fused octahydroquinolizine skeleton.[7] Moreover, both clusters (A and B) showed good anti-HCV activity, and the cluster A derivatives (±)-13*α*-methoxymyrifabral A (**5**), (±)-13*β*-methoxymyrifabral A (**6**), and (±)-dehydratedmyrifabral A (**7**) exhibited improved activity in comparison to the parent structures. These active frameworks may benefit future efforts to develop anti-HCV compounds. In this paper, we report the structural elucidation and chiral separation of **1**−**4**. We propose a biosynthetic pathway, prepare derivatives of the natural products, and evaluate the anti-HCV activity of **1**−**7**.

RESULTS AND DISCUSSION

M. faberi is a wild herb from China.[8] The aerial parts of *M. faberi* were collected after flowering in the Sichuan province of the People's Republic of China in October 2011. The air-dried, powdered leaves and stems (30 kg) of *M. faberi* were extracted three times with 50 L of 95% EtOH. After removal of saccharides by passing through macroporous resin (D101), the

Received: May 19, 2014
Published: August 7, 2014

   dx.doi.org/10.1021/jo501076x | J. Org. Chem. 2014, 79, 7945−7950

crude extract (223 g) was subjected to normal-phase silica gel chromatography (200−300 mesh; $CHCl_3$/MeOH, 20/1 → 0/1) to afford four fractions (Fr 1−4). Fr 4 (25 g) was further separated on normal-phase silica gel (200−300 mesh; $CHCl_3$/MeOH/diethylamine, 30/1/0.01) into four subfractions (Fr 4A-4D). Fr 4B (1.2 g) was subjected to Sephadex LH-20 CC with $CHCl_3$/MeOH 1/1 as eluent and further purified using normal-phase silica gel (300−400 mesh; $CHCl_3$/MeOH/diethylamine, 30/1/0.01) to yield clusters A (**1** and **2**; 30 mg) and B (**3** and **4**; 2 mg) (Figure 1).

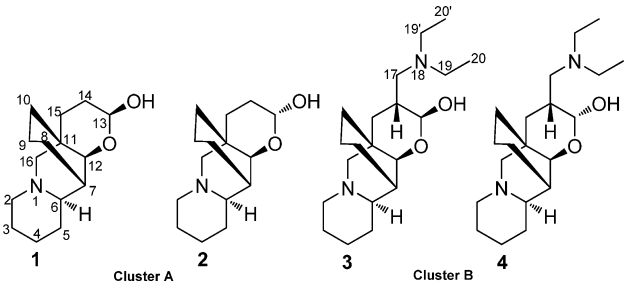

Figure 1. Structures of **1**−**4**.

The 1D-NMR spectrum of cluster A (**1** and **2**) showed two groups of distinguishable signals (Figures S1.1 and S1.2 in the Supporting Information). The downfield positions of the carbon atoms (δ_C 98.3 in **1** and δ_C 92.3 in **2**) suggested the atoms to be dioxygenated, and the ^{13}C NMR chemical shifts of **1** and **2** mainly differ at the positions close to C-13, which indicated these two structures to be epimers at C-13. Accordingly, they were recognized to be hemiacetals with interconversion equilibrium, similar to dihydroartemisinin[9] and other inseparable hemiacetals[10] (Tables 1 and 2).

Compounds **1** and **2** in cluster A are isomers. Their identical molecular formulas were established as $C_{15}H_{25}NO_2$ by HREIMS: $[M]^+$ m/z found 251.1892; calcd for $C_{15}H_{25}NO_2$ 251.1885. On the basis of this formula, **1** and **2** had four degrees of unsaturation. The ^{13}C NMR and DEPT spectra of the mixture of **1** and **2** (Figure S1.2 in the Supporting Information) revealed 30 carbon signals: 2 × (10 × CH_2, 4 × CH, 1 × qC) (Figure 1).

Table 1. ^{13}C NMR Data (ppm) for 1−4 Recorded in Pyridine-d_5 at 125 MHz

no.	1	2	3	4
2	57.2 (CH_2)	57.2 (CH_2)	57.0 (CH_2)	57.1 (CH_2)
3	25.4 (CH_2)	25.4 (CH_2)	25.2 (CH_2)	25.3 (CH_2)
4	26.8 (CH_2)	26.9 (CH_2)	26.7 (CH_2)	26.8 (CH_2)
5	30.6 (CH_2)	30.7 (CH_2)	30.3 (CH_2)	30.4 (CH_2)
6	66.4 (CH)	66.8 (CH)	66.3 (CH)	66.7 (CH)
7	40.4 (CH)	40.1 (CH)	39.9 (CH)	39.8 (CH)
8	21.2 (CH_2)	21.3 (CH_2)	21.1 (CH_2)	21.1 (CH_2)
9	21.3 (CH_2)	21.4 (CH_2)	21.3 (CH_2)	21.4 (CH_2)
10	29.6 (CH_2)	28.7 (CH_2)	30.5 (CH_2)	29.7 (CH_2)
11	32.6 (qC)	33.0 (qC)	33.7 (qC)	33.6 (qC)
12	80.6 (CH)	72.5 (CH)	80.2 (CH)	72.7 (CH)
13	98.3 (CH)	92.3 (CH)	103.0 (CH)	94.0 (CH)
14	30.5 (CH_2)	29.5 (CH_2)	37.1 (CH)	35.0 (CH)
15	34.4 (CH_2)	30.6 (CH_2)	38.9 (CH_2)	35.0 (CH_2)
16	69.0 (CH_2)	69.6 (CH_2)	68.9 (CH_2)	69.6 (CH_2)
17			56.6 (CH_2)	56.9 (CH_2)
19			47.8 (CH_2)	48.3 (CH_2)
20			12.2 (CH_3)	12.7 (CH_3)

The two-dimensional structure of **1** was established by 2D NMR ($^1H-^1H$ COSY, HSQC, and HMBC), on the basis of the elucidation of three subunits: parts A and B and a linkage (Figure 2). The dioxygenated methine was easily recognized (C-13, δ_C 98.3). The identity of the hemiacetal group was supported by HMBC correlations from H-12 (δ_H 3.21, d, 3.6 Hz) to C-13. The structure of part A was deduced from the HMBC correlations from H_2-14 (δ_H 2.00, m; 1.22, m) and H_2-15 (δ_H 1.23, m) to C-11 (δ_C 32.6) and the presence of a $^1H-^1H$ spin system involving H-13 (δ_H 5.12, dd, 9.6, 2.4 Hz), H_2-14, and H_2-15. Meanwhile, the structure of part B was elucidated from a $^1H-^1H$ spin system (H_2-2/H_2-3/H_2-4/H_2-5/H_2-6 and HMBC) and the correlations from H_2-2 (δ_H 2.68, m; 1.62, m) to C-6 (δ_C 66.4) and from H_2-16 (δ_H 2.54, m; 1.74, m) to C-2 (δ_C 57.2) and C-6. As a result, the linkage between parts A and B through C-7 (δ_C 40.4) and C-16 (δ_C 69.0) was confirmed from the $^1H-^1H$ spin system H-6/H-7/H-12 and by HMBC correlations from H_2-16 to C-11 (δ_C 32.6) and C-12 (δ_C 80.6) and from H-12 to C-6 and C-16. Finally, the remaining three methylenes were assigned to a bridge between C-7 and C-11, which can be supported by the $^1H-^1H$ COSY fragment of H-8/H-9/H-10 and HMBC correlation from H-12 to C-10 (δ_C 29.6). Thus, the two-dimensional structure of **1** was determined to be that shown in Figure 2. In a similar manner, **2** was determined to be 13-*epi*-**1**, possessing the same two-dimensional structure.

To confirm the structures of **1** and **2**, cluster A was recrystallized from methanol for an X-ray diffraction experiment. Only crystals of **2** were obtained; it was shown to be a racemate by its space group $P2_1/c$.[11] As a result, the structure of **2** was assigned as that shown (Figure 3). The methylated derivatives of **1** and **2** (**5** and **6**, respectively) exhibited four peaks by chiral HPLC (Figure 6); thus, **1** was also shown to be a racemate. The NMR data of **1** and **2** differed in a ROESY correlation between H-12 and H-13 (detected in **1** but not in **2**) (Figure S1.6 in the Supporting Information). The molar ratio **1**:**2** (1:0.61 in pyridine-d_5) was calculated from the ^1H NMR integration.

Compounds **3** and **4** were also isolated as pairs of epimers. Their identical molecular formulas were established as $C_{20}H_{36}N_2O_2$ by HREIMS ($[M]^+$ m/z 336.2781, calcd for $C_{20}H_{36}N_2O_2$ 336.2777), corresponding to four degrees of unsaturation. The 1D NMR spectra of **3** and **4** exhibited high similarity to those of **1** and **2** but had three additional carbon signals (C-17, C-19/C-19′, C-20/C-20′).Two downfield methine signals (δ_C 103.0 in **3** and δ_C 94.0 in **4**) were recognized as typical of hemiacetals (Table 1). The existence of two $-CH_2CH_3$ fragments ($C_{19,20}$ and $C_{19',20'}$) was indicated by the ^1H NMR coupling constants and integration (H_3-20 δ_H 0.98 (6H, t, J = 6.6 Hz) in **3**; H_3-20 δ_H 1.02 (6H, t, J = 6.6 Hz) in **4**). The connection of these fragments to a nitrogen atom was suggested by the relatively high field shift of H_2-19 (δ_H 2.39, m in **3**; δ_H 2.51, m in **4**) (Figure 4).

Further analysis of the 2D NMR spectra of **3** ($^1H-^1H$ COSY, HSQC, and HMBC; Figure 4) revealed its structural similarity with **1**. HMBC correlations from H_2-2 (δ_H 2.68, m; 1.63, m) to C-6 (δ_C 66.3) and C-16 (δ_C 68.9), from H_2-16 (δ_H 2.58, m; 1.79, m) to C-6 and C-12 (δ_C 80.2), and from H-12 (δ_H 2.24, d, 3.6 Hz) to C-6 suggested the presence of an octahydroquinolizine. A six-membered hemiacetal ring was indicated by HMBC correlations from H-12 to C-13 and C-15 (δ_C 38.9) and from

dx.doi.org/10.1021/jo501076x | J. Org. Chem. 2014, 79, 7945−7950

Table 2. ^{1}H NMR Data (ppm) for 1−4 Recorded in Pyridine-d_5 at 600 MHz

no,	1	2	3	4
2	2.68 (m)	2.68 (m)	2.68 (m)	2.68 (m)
	1.62 (m)	1.62 (m)	1.63 (m)	1.63 (m)
3	1.64 (m)	1.64 (m)	1.63 (m)	1.63 (m)
	1.14 (m)	1.14 (m)	1.14 (m)	1.14 (m)
4	1.46 (m)	1.46 (m)	1.46 (m)	1.46 (m)
5	2.00 (m)	2.07 (m)	2.27 (m)	2.27 (m)
	1.50 (m)	1.76 (m)	1.29 (m)	1.29 (m)
6	1.89 (m)	1.95 (m)	1.94 (m)	1.94 (m)
7	1.74 (m)	1.66 (m)	1.80 (m)	1.71 (m)
8	2.03 (m)	1.97 (m)	2.05 (m)	2.05 (m)
	1.64 (m)	1.64 (m)	1.66 (m)	1.66 (m)
9	2.69 (m)	2.74 (m)	2.71 (m)	2.78 (m)
	1.43 (m)	1.48 (m)	1.46 (m)	1.53 (m)
10	2.23 (m)	2.26 (m)	2.28 (m)	2.36 (m)
	1.18 (m)	1.20 (m)	1.30 (m)	1.32 (m)
12	3.21 (d, 3.6)	4.21 (d, 4.8)	3.24 (d, 3.6)	4.23 (d, 3.0)
13	5.12 (dd, 9.6, 2.4)	5.70(d, 3.6)	4.83 (d, 8.4)	5.74 (d, 2.4)
14	2.00 (m)	2.23 (m)	2.12 (m)	2.40 (m)
	1.22 (m)	1.07 (m)		
15	1.23 (m)	1.50	1.39 (dd, 13.2, 4.2)	1.50 (m)
		1.23 (m)	0.84 (m)	1.30 (dd, 13.6, 5.4)
16	2.54 (m)	2.54 (m)	2.58 (m)	2.58 (m)
	1.74 (m)	1.92 (m)	1.79 (m)	1.97 (m)
17			2.68 (m)	2.78 (m)
			2.20 (dd, 12.6, 6.0)	2.37 (m)
19			2.39 (m)	2.51 (m)
20			0.98 (t, 6.6)	1.02 (t, 6.6)

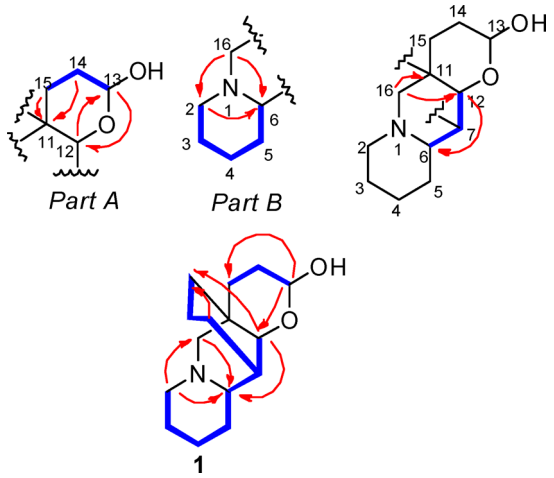

Figure 2. ^{1}H−^{1}H COSY and key HMBC correlations of 1.

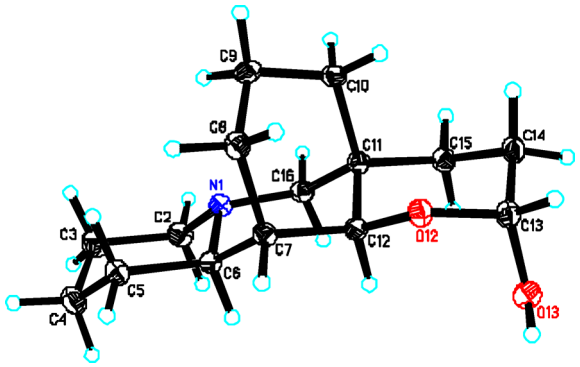

Figure 3. Crystal structure of (±)-α-myrifabral A (2).

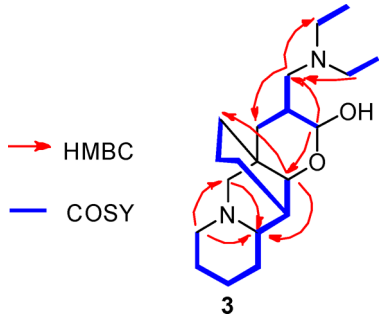

Figure 4. ^{1}H−^{1}H COSY and key HMBC correlations of 3.

H-13 (δ_H 4.83, d, 8.4 Hz) to C-15 and C-12. The connection of the diethylamine fragment to the tetracyclic framework through C-17 (δ_C 56.6) was identified by the HMBC correlations from H_2-19 to C-17, from H_2-17 (δ_H 2.68, m; 2.20, dd, 12.6, 6.0 Hz) to C-13 and C-15, and from H-13 to C-15 and C-17 (Figure 4).

To establish the stereochemistry of 3 and 4 and to check whether cluster B was also racemic, X-ray diffraction analysis was utilized. Cluster B was recrystallized from methanol to afford a cocrystal suitable for X-ray diffraction. The final refinement of the Mo Kα data provided the structures of 3 and 4 shown in Figure 5 and also revealed 3 and 4 to be racemates by the space group $P\bar{1}$.[11] The NMR data of 3 and 4 differed in a ROESY correlation between H-12 and H-13 (detected in 3 but not in 4) (Figure S2.6 in the Supporting Information). The ratio 3:4 in the unit cell was 1:0.78, as calculated by X-ray crystallographic analysis.[12]

dx.doi.org/10.1021/jo501076x | J. Org. Chem. 2014, 79, 7945−7950

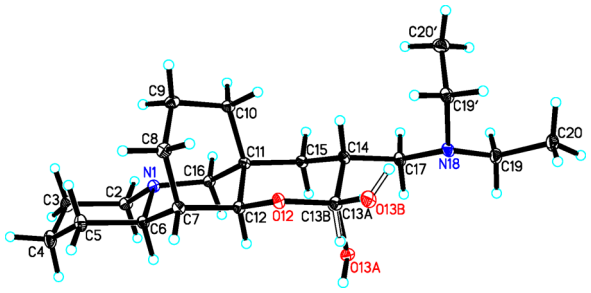

Figure 5. Cocrystal structure of (±)-*β*-myrifabral B (**3**) and (±)-*α*-myrifabral B (**4**).

In most cases, chiral natural products are produced in optically pure form, with only one enantiomer biosynthesized.[13] Infrequently, enantiomeric metabolites have also been reported, but at a low occurrence of less than 1% relative to the overall abundance of natural products.[14]

The decahydroquinoline (DHQ) motif is a common feature of *Myrioneuron* alkaloids,[7] but **1**−**4** are exceptions. An octahydroquinolizine (OHQ) core in L-lysine-derived quinolizidine alkaloids is found primarily in the Fabaceae and Lycopodiaceae families.[15] Thus, the OHQ core fused with a cyclohexane fragment in **1**−**4** represents a novel skeleton and suggests an atypical biosynthetic pathway for **1**−**4**, different from those for the other quinolizidine and *Myrioneuron* alkaloids.

A proposed biosynthetic pathway for **1**−**4** starting from L-lysine[7c,16] is shown in Scheme 1. The C_5 building blocks **A** and

Scheme 1. Proposed Biosynthetic Pathway for 1−4

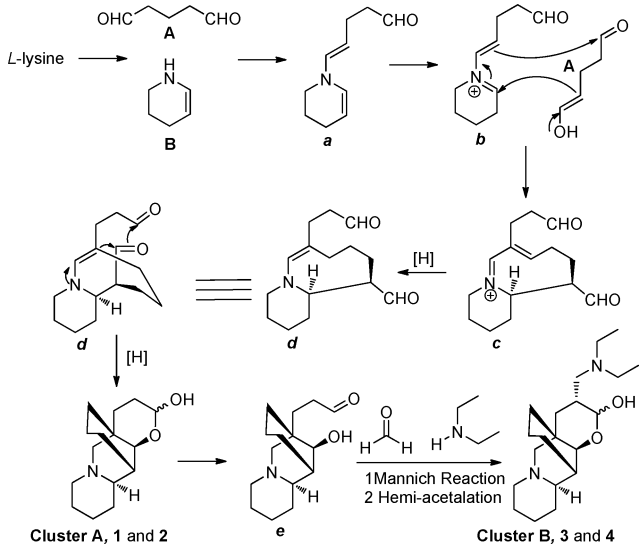

B could be derived from L-lysine through decarboxylation, oxidation, and cyclization.[17] Condensation of **A** and **B** could yield intermediate ***a***, which would afford conjugated structure ***b*** after double-bond migration. The key intermediate ***c*** could be formed by a Michael addition between ***b*** and **A**, and ***c*** could then be reduced to ***d***. Subsequently, cluster A, as a mixture of **1** and **2**, could be derived from ***d*** by intramolecular condensation and hemiacetalization. Finally, cluster B (**3** and **4**) could be produced through a Mannich reaction among ***e***, formaldehyde,[18] and diethylamine[19] and subsequent hemiacetalization.

To provide further evidence, cluster A (20 mg of **1** and **2**) was converted to acetals **5** (5 mg) and **6** (8 mg), which were separated, as shown in Scheme 2 (for NMR data see Table 3).

Scheme 2. Derivatives of Cluster A and Their Separation

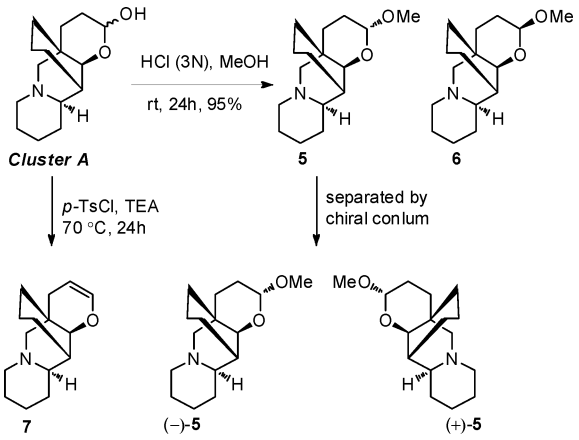

Then (+)-**5** and (−)-**5** were separated by chiral HPLC; resolution of (±)-**6** was attempted using five types of chiral columns, but all were unsuccessful (Figure 6). Cluster A (6 mg) was similarly converted to **7** (5 mg), but resolution was also unsuccessful. Due to the small amount of cluster B (2 mg) obtained, acetal formation was unsuccessful.

Clusters A and B and derivatives **5**−**7** were tested for anti-HCV activity.[7f,g] All tested alkaloids exhibited less cytotoxicity against liver cells than the positive control telaprevir (VX-950). Derivatives **5**−**7** showed enhanced activity in comparison to their parent compounds; **5** was the most active and had a selectivity index (SI; CC_{50}/IC_{50}) of 160.9 (Table 4).

EXPERIMENTAL SECTION

General Experimental Procedures. Melting points were measured on a digital melting point apparatus. 1D and 2D NMR spectra were run on 600 MHz NMR spectrometers for ^{1}H and 150 MHz spectrometers for ^{13}C with TMS as the internal standard. ESIMS and HREIMS were carried out with a time-of-flight spectrometer. Column chromatography (CC) was performed on silica gel (200−300 and 100−200 mesh) and Sephadex LH-20 (40−70 *μ*m). HPLC was performed with an HPLC equipped with a DAD detector.

Cluster A (1 and 2): colorless crystal, mp 149−150 °C; $[\alpha]_D^{19}$ = −5° (*c* 0.35, MeOH); UV (MeOH) λ_{max} (log ε) 207 nm (2.85); ^{13}C and ^{1}H NMR data, Tables 1 and 2; positive ESIMS *m*/*z* 252 [M + H]$^+$, 274 [M + Na]$^+$; positive HREIMS *m*/*z* 251.1892 [*M*]$^+$, calcd for $C_{15}H_{25}NO_2$ 251.1885.

Cluster B (3 and 4): colorless crystal, mp 131−132 °C; $[\alpha]_D^{22}$ = −15° (*c* 0.10, MeOH); UV (MeOH) λ_{max} (log ε) 204 nm (2.90); ^{13}C and ^{1}H NMR data, Tables 1 and 2; positive ESIMS *m*/*z* 337 [M + H]$^+$; positive HREIMS *m*/*z* 336.2781 [*M*]$^+$, calcd for $C_{20}H_{36}N_2O_2$, 336.2777.

(±)-13*α*-Methoxy-myrifabral A (5) and (±)-13*β*-Methoxy-myrifabral A (6). A solution of cluster A (**1** and **2**; 20 mg) in MeOH (8.0 mL) was placed in a round-bottomed flask, followed by addition of concentrated hydrochloric acid (HCl 37%, 2.0 mL). The mixture was stirred at room temperature for 24 h, and then saturated $NaHCO_3$ (10.0 mL) was added slowly. The reaction solution was evaporated to remove MeOH and extracted with CH_2Cl_2 (10 mL) twice. The organic layers were combined and concentrated. The products were separated by HPLC with MeCN/H_2O (3/7) to give **5** (5 mg) and **6** (8 mg) as amorphous powders: ^{1}H and ^{13}C NMR data, Table 3; positive ESIMS *m*/*z* 266 [M + H]$^+$; positive HREIMS *m*/*z* 265.2043 [*M*]$^+$, calcd for $C_{16}H_{27}NO_2$ 265.2042.

dx.doi.org/10.1021/jo501076x | J. Org. Chem. 2014, 79, 7945−7950

Table 3. ^{1}H and ^{13}C NMR Data for 5 and 6 Recorded in Pyridine-d_5 at 600 and 125 MHz, Respectively

	5			6		
		δ_H			δ_H	
no.	δ_C			δ_C		
2	56.4	2.63 (d, 10.4)	1.58 (m)	56.4	2.64 (m)	1.59 (m)
3	24.7	1.60 (m)	1.13 (m)	24.7	1.60 (m)	1.13 (m)
4	26.1	1.44 (m)		26.1	1.43 (m)	
5	25.6	1.88 (m)	1.55 (m)	29.8	1.57 (m)	1.47 (m)
6	66.0	1.88 (m)		65.6	1.88 (m)	
7	39.0	1.58 (m)		39.3	1.63 (m)	
8	20.3	1.88 (m)	1.60 (m)	20.4	1.88 (m)	1.56 (m)
9	20.5	2.68 (m)	1.43 (m)	20.5	2.63 (m)	1.37 (m)
10	27.9	2.11 (m)	1.13 (m)	28.8	2.11 (tdd, 12.8, 6.4, 2.4)	1.11 (m)
11	32.0	2.67 (m)	1.44 (m)	32.0		
12	72.2	3.58 (m)		79.8	3.04 (d, 3.2)	
13	98.5	4.79 (m)		104.2	4.38 (dd, 9.6, 2.4)	
14	29.0	1.52 (m)	0.95 (dd, 12.8, 4.0)	27.7	1.79 (tdd, 13.6, 8.8, 4.8)	1.60 (m)
15	29.9	2.48 (m)	1.23 (d, 12.8)	33.2	1.14 (m)	1.10 (m)
16	68.6	2.44 (d, 11.2)	1.78 (d, 11.2)	68.2	2.49 (d, 11.2)	1.69 (dd, 11.2, 2.4)
17	54.0	3.36 (s)		55.6	3.54 (s)	

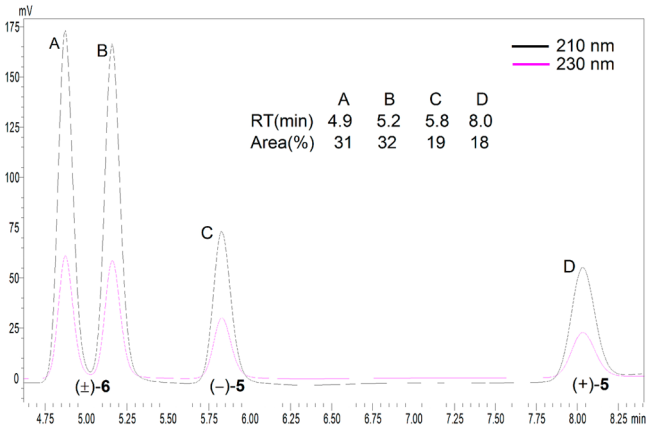

Figure 6. Analysis of a mixture of (±)-5 and (±)-6 by chiral HPLC (OD-H 4.6 × 150 mm, *n*-hexane, 1.0 mL/min).

Table 4. Anti-HCV Bioassay Results[a]

compd	CC_{50} (μM)	EC_{50} (μM)	SI
cluster A	119.1	4.7	25.3
cluster B	169.3	2.2	77.0
5	144.8	0.9	160.9
6	184.9	1.6	115.6
7	134.8	1.7	79.3
VX-950	32.5	0.09	361.1

[a]VX-950 as positive control.

(±) -Dehydrated-myrifabral A (7). A solution of cluster A (**1** and **2**; 6 mg) in CH_2Cl_2 (6.0 mL) was placed in a sealable tube, followed by addition of triethylamine (TEA; 20 μL) and 4-toluene sulfonyl chloride (*p*-TsCl; 6.0 mg). The mixture was stirred in the sealed tube at 70 °C for 24 h and then cooled to room temperature. The reaction solution was then diluted with 6 mL of water and extracted twice. The organic layers were combined and concentated. The residue was purified by column chromatography with $CHCl_3$/MeOH/diethylamine 40/1/0.01 as eluent to give **7** (5 mg) as an amorphous powder: positive ESIMS *m*/*z* 234 $[M + H]^+$; positive HREIMS *m*/*z* 233.1785 $[M]^+$, calcd for $C_{15}H_{23}NO$ 233.1780.

Cells. Huh7.5 human liver cells (kindly provided by Vertex Pharmaceuticals, Boston, MA) were cultured in Dulbecco's Modified Eagle's Medium (DMEM, Invitrogen, CA) supplemented with 10% inactivated fetal bovine serum (Invitrogen) and 1% penicillin-streptomycin (Invitrogen). Cells were cultured at 37 °C in 5% CO_2.

HCV Infection and Treatment. The Huh7.5 cells were seeded into 96-well plates (Costar) at a density of 3×10^4 cells/cm^2; after 24 h incubation, cells were infected with HCV (approximately 45 IU per cell) and simultaneously treated with cluster A or B, **5**−**7**, or solvent control. The culture medium was removed 72 h after inoculation, and intracellular RNA was extracted with an RNeasy Mini Kit. Intracellular RNA from HCV and the internal control gene glyceraldehyde 3-phosphate dehydrogenase (GAPDH) were quantified with an AgPath-ID One-Step RT-PCR Kit. The results were calculated using the $2^{\Delta\Delta CT}$ method.[20] The half-maximum effective concentration (EC_{50}) was calculated using the method of Reed and Muench.[21]

X-ray Crystal Structure Analysis. A colorless crystal of **2** and colorless cocrystals of **3** and **4** were obtained from methanol. Intensity data for **2** were collected using Cu Kα radiation, while those for **3** and **4** were collected using Mo Kα radiation. The structure was solved by direct methods using SHELXL-97.[22] Refinements were performed using the full-matrix least-squares method, with anisotropic displacement parameters for all non-hydrogen atoms. H atoms were placed in calculated positions and refined using a riding model. Compound **2**: colorless crystal, mp 149−150 °C, $C_{15}H_{25}NO_2$, M_r = 251.36, monoclinic, a = 10.5931(5) Å, b = 12.4309(6) Å, c = 10.6076(5) Å, α = 90.00°, β = 105.109(2)°, γ = 90.00°, V = 1348.54(11) Å^3, T = 100(2) K, space group $P2_1/c$, Z = 4, μ(Cu Kα) = 0.637 mm^{-1}, 9196 reflections measured, 2334 independent reflections (R_{int} = 0.0360). The final R1 value was 0.0568 ($I > 2\sigma(I)$). The final wR2(F^2) value was 0.1525 ($I > 2\sigma(I)$). The final R1 value was 0.0579 (all data). The final wR2(F^2) value was 0.1535 (all data). The goodness of fit on F^2 was 1.091. Crystallographic data (excluding structure factor tables) for **2** have been deposited with the Cambridge Crystallographic Data Center (CCDC 926408). Cocrystal of **3** and **4**: colorless crystal, mp 131−132 °C, $C_{20}H_{36}N_2O_2$, M_r = 336.51, triclinic, a = 8.6049(16) Å, b = 9.2797(17) Å, c = 11.975(2) Å, α = 86.715(3)°, β = 76.606(2)°, γ = 87.794(3)°, V = 928.3(3) Å^3, T = 100(2) K, space group $P\bar{1}$, Z = 2, μ(Mo Kα) = 0.077 mm^{-1}, 12341 reflections measured, 5005 independent reflections (R_{int} = 0.0378). The final R1 value was 0.0476 ($I > 2\sigma(I)$). The final wR2(F^2) value was 0.1220 ($I > 2\sigma(I)$). The final R1 value was 0.0637 (all data). The final wR2(F^2) value was 0.1338 (all data). The goodness of fit on F^2 was 1.071. Crystallographic data have been deposited at the Cambridge Crystallographic Data Center (CCDC 909194). Copies of the data can be obtained free of charge by application to the CCDC, 12 Union Road, Cambridge CB

dx.doi.org/10.1021/jo501076x | J. Org. Chem. 2014, 79, 7945−7950

1EZ, U.K. (fax, int. +44 (0) (1223) 336 033; e-mail, deposit@ccdc.cam.ac.uk).

■ ASSOCIATED CONTENT

Supporting Information

Figures, tables, and CIF files giving 1D and 2D NMR, ESIMS and HRESIMS spectra for **1**−**6**, 1D NMR, ESIMS, and HRESIMS spectra for **7**, and X-ray crystallographic data for **2**−**4**. This material is available free of charge via the Internet at http://pubs.acs.org.

■ AUTHOR INFORMATION

Corresponding Author

*X.-J.H.: tel, +86-871-65223263; fax, +86-871-65223070; e-mail, haoxj@mail.kib.ac.cn.

Notes

The authors declare no competing financial interest.

■ ACKNOWLEDGMENTS

This research was supported financially by the National Natural Science Foundation of China (21372228), the Foundation of Chinese Academy of Sciences (Y.Z.), and a Syngenta postgraduate studentship (M.-M.C., 2012−2015). We are grateful to Dr. James D. Simo Mpetga (University of Dschang) for linguistic improvement.

■ REFERENCES

(1) WHO. Hepatitis C. Fact sheet No. 164 2014; www.who.int/mediacentre/factsheets/fs164/en/ (updated April 2014).

(2) (a) Zeuzem, S. *Nat. Clin. Pract. Gastroenterol. Hepatol.* **2008**, *5*, 610−622. (b) McHutchison, J. G.; Lawitz, E. J.; Shiffman, M. L.; Muir, A. J.; Galler, G. W.; et al. *N. Engl. J. Med.* **2009**, *361*, 580−593.

(3) Thompson, A. J.; McHutchison, J. G. *J. Viral Hepat.* **2009**, *16*, 377−387.

(4) Afdhal, N. H.; Zeuzem, S.; Schooley, R. T.; Thomas, D. L.; Ward, J. W.; Litwin, A. H.; Razavi, H.; Castera, L.; Poynard, T.; Muir, A.; Mehta, S. H.; Dee, L.; Graham, C.; Church, D. R.; Talal, A. H.; Sulkowski, M. S.; Jacobson, I. M. *J. Viral Hepat.* **2013**, *20*, 745−760.

(5) Ghany, M. G.; Strader, D. B.; Thomas, D. L.; Seeff, L. B. *Hepatology* **2009**, *49*, 1335−1374.

(6) Newman, D. J.; Cragg, G. M. *J. Nat. Prod.* **2012**, *75*, 311−335.

(7) (a) Pham, V. C.; Jossang, A.; Chiaroni, A.; Sévenet, T.; Bodo, B. *Tetrahedron Lett.* **2002**, *43*, 7565−7568. (b) Pham, V. C.; Jossang, A.; Chiaroni, A.; Sévenet, T.; Nguyen, V. H.; Bodo, B. *Org. Lett.* **2007**, *9*, 3531−3534. (c) Pham, V. C.; Jossang, A.; Grellier, P.; Chiaroni, A.; Sévenet, T.; Nguyen, V. H.; Bodo, B. *J. Org. Chem.* **2008**, *73*, 7565−7573. (d) Pham, V. C.; Jossang, A.; Sévenet, T.; Nguyen, V. H.; Bodo, B. *Eur. J. Org. Chem.* **2009**, *74*, 1412−1416. (e) Pham, V. C.; Jossang, A.; Sévenet, T.; Nguyen, V. H.; Bodo, B. *Tetrahedron* **2007**, *63*, 11244−11249. (f) Huang, S.-D.; Zhang, Y.; Cao, M.-M.; Di, Y.-T.; Tang, G.-H.; Peng, Z.-G.; Jiang, J.-D.; He, H.-P.; Hao, X.-J. *Org. Lett.* **2013**, *15*, 590−593. (g) Cao, M.-M.; Huang, S.-D.; Di, Y.-T.; Yuan, C.-M.; Zuo, G.-Y.; Gu, Y.-C.; Zhang, Y.; Hao, X.-J. *Org. Lett.* **2014**, *16*, 528−531.

(8) Luo, X.-R.; Gao, Y.-Z.; Chen, W.-Q.; Xu, X.-H.; Wu, H. *Flora of China* **1999**, *71*, 310−312.

(9) Pathak, A. K.; Jain, D. C.; Sharma, R. P. *Indian J. Chem. B* **1995**, *11*, 992−993.

(10) (a) Bates, R. B.; Haber, W. A.; Setzer, W. N.; Stessman, C. C. *J. Nat. Prod.* **1999**, *62*, 340−341. (b) Kwon, Y.-J.; Sohn, M.-J.; Kim, C.-J.; Koshino, H.; Kim, W.-G. *J. Nat. Prod.* **2012**, *75*, 271−274.

(11) Chen, X.-M.; Cai, J.-W. In *The Principle and Practice of Single Crystal Sructure Analysis*; Science Press: Beijing, 2003; pp 23−36.

(12) Wu, H.-K.; Fronczek, F. R.; Ferreira, D.; Burandt, C. L., Jr; Zjawiony, J. K. *J. Nat. Prod.* **2011**, *74*, 831−836.

(13) Miller, K. A.; Tsukamoto, S.; Williams, R. M. *Nat. Chem.* **2009**, *1*, 63−68.

(14) Finefield, J. M.; Sherman, D. H.; Kreitman, M.; Williams, R. M. *Angew. Chem., Int. Ed.* **2012**, *51*, 4802−4836.

(15) Michael, J. P. *Nat. Prod. Rep.* **2008**, *25*, 139−165.

(16) (a) Wanner, M. J.; Koomen, G. J. *Pharmacochem. Libr.* **1997**, *28*, 179−187. (b) Golebiewski, W. M.; Spenser, I. D. *J. Am. Chem. Soc.* **1976**, *98*, 6726−6728. (c) Gravel, E.; Harfouche, A.; Salame, R.; Leblanc, K.; Maciuk, A.; Poupon, E. *Chem. Eur. J.* **2013**, *19*, 14515−14520. (d) Gravel, E.; Poupon, E.; Hocquemiller, R. *Org. Lett.* **2005**, *7*, 2497−2499.

(17) (a) Francois, D.; Lallemand, M.-C.; Selkti, M.; Tomas, A.; Kunesch, N.; Husson, H.-P. *Angew. Chem., Int. Ed.* **1998**, *37*, 104−105. (b) Wanner, M. J.; Koomen, G.-J. *J. Org. Chem.* **1995**, *60*, 5634−5637.

(18) The formaldehyde may result from microbial degradation reactions: Dewick, P. M. In *Medicinal Natural Products: A Biosynthetic Approach*, 3rd ed.; Wiley: Chichester, U.K., 2009; pp 163−165.

(19) The diethylamine may be introduced artificially during the separation procedures.

(20) Livak, K. J.; Schmittgen, T. D. *Methods* **2001**, *25*, 402−4−8.

(21) (a) Reed, L. J.; Muench, H. A. *Am. J. Hyg.* **1938**, *27*, 493−497. (b) Peng, Z.-G.; Fan, B.; Du, N.-N.; Wang, Y.-P.; Gao, L.-M.; Li, Y.-H.; You, X.-F.; Han, Y.-X.; Zhao, Z.-Y.; Cen, S.; Li, J.-R.; Song, D.-Q.; Jiang, J.-D. *Hepatology* **2010**, *52*, 845−853.

(22) Sheldrick, G. M. *SHELXL97*; University of Göttingen, Göttingen, Germany, 1997.